ICES Journal of Marine Science, 2023, **0**, 1–14
DOI: 10.1093/icesjms/fsad094
Original Article

Mining previous acoustic surveys to improve walleye pollock (*Gadus chalcogrammus*) target strength estimates

N. Lauffenburger *, A. De Robertis and K. Williams

Alaska Fisheries Science Center, National Marine Fisheries Service, National Oceanic and Atmospheric Administration, 7600 Sand Point Way NE Seattle, WA 98115 , USA

* *Corresponding author:tel: +1 206 526 4177;* e-mail: nathan.lauffenburger@noaa.gov.

Acoustic-trawl surveys are widely used to measure the abundance and distribution of pelagic fish. The echo integration method used in these surveys requires estimates of the target strength (TS, dB re 1 m^2) of acoustic scatterers. Here, we present a new automated method to estimate TS from a large volume of previously collected acoustic survey data recorded near trawl sites. By applying a series of selection and filtering methods to echosounder data, single echo measurements representative of fish encountered during surveys can be objectively and reliably isolated from existing survey data. We applied this method to 30 surveys of walleye pollock (*Gadus chalcogrammus*) conducted in Alaska from 2007 to 2019 and estimated a new length-to-TS relationship. The resulting relationship ($TS = 20.0 \cdot \log_{10} L - 66.0$) was largely consistent with previous *in situ* estimates made during dedicated, mostly nighttime TS collection events. Analysis of this sizeable data set ($n = 142$) indicates that increased fish depth, lower ambient temperature, and summer months may increase pollock TS. The application of a new TS model incorporating these environmental covariates to historic surveys resulted in -16 to +21% changes in abundance relative to the model without environmental covariates. This study indicates that useful TS measurements can be uncovered from existing datasets.

Keywords: acoustic backscatter, acoustic trawl survey, biomass.

Introduction

Acoustic-trawl (AT) surveys are widely used to assess the abundance and distribution patterns of pelagic fish. In these surveys, acoustic backscatter is combined with species and length information from trawl samples to calculate fish abundance (Simmonds and MacLennan, 2008). Abundance estimates are typically based on the echo integration method (Foote, 1983), which depends on knowledge of the backscatter from an individual fish, referred to as the backscattering cross-section (σ_{bs}, m^2) or the more commonly used logarithmic counterpart, target strength (TS, dB re 1 m^2; MacLennan *et al.*, 2002). While TS is predominantly influenced by fish species and size, it may also be influenced by physiology (e.g. maturity and condition) and the behaviour of the fish as encountered *in situ* (e.g. depth and orientation; Miyanohana *et al.*, 1990; Horne, 2003). Fish abundance estimates are directly proportional to these TS estimates, and an increased understanding of the TS relationship will reduce uncertainties in survey abundance estimates.

Historically, empirical- and model-based approaches have been used to measure the TS of fish and other acoustic scatterers. TS measurements of fish and synthetic targets have been made in tank experiments, which have the benefit of known length and orientation of the targets (Love, 1971; Midttun, 1984; Foote and Ona, 1985; Sawada *et al.*, 1999; Hazen and Horne, 2004; Cotter *et al.*, 2021; Yoon *et al.*, 2023). Similarly, mathematical models have been developed and parametrized based on the morphology and material properties of the organisms (Foote and Francis, 2002; Hazen and Horne, 2004; Fässler *et al.*, 2009; Jech *et al.*, 2015). While the relationship between animal orientations (or degree of tilt) and their TS within a tank or based on a model can be established, the effect of fish behaviour (which affects TS via changes in orientation and swim bladder inflation) under survey conditions is generally unknown. Further, differences in season, depth, maturity state, and stomach fullness may influence the TS (Ona, 1990), but are difficult to assess in laboratory measurements and models. Thus, many attempts have been made to examine the distribution of TSs *in situ* (Foote, 1991; Traynor, 1996; McQuinn and Winger, 2003; Zhao *et al.*, 2008; Rose, 2009; Cotter *et al.*, 2021), as these measurements are likely to most closely represent survey conditions. However, measuring TS *in situ* presents a number of challenging limitations. Resolving echoes from individual fish and determining the corresponding species and size of the TS targets is difficult. Often, lowered echo sounders have been used to get closer to targets in an effort to isolate individuals in high-density aggregations (Dalen and Bodholt, 1991; Pedersen *et al.*, 2011) and reduce range-dependent noise biases (Kieser *et al.*, 2005).

An alternative approach to develop a more accurate *in situ* estimate of a species' TS is to examine the information contained in existing AT survey time series rather than only the data from dedicated TS collection events. Such surveys constitute large data sets over many years with calibrated acoustic observations and trawl samples to verify the identity of the acoustic scatterers. A subset of these observations that meet specific single target criteria may be suitable for the determination of *in situ* TS under survey conditions. A key advantage of deriving TS measurements from existing survey data is that the resulting TS estimates will be more representative of the collection conditions and fish distributions experienced during the surveys. Additionally, re-analysis of existing survey data is cost-effective as it does not require dedicated ship time for TS observations.

Received: 13 March 2023; **Revised:** 17 May 2023; **Accepted:** 18 May 2023

Large AT survey data sets can be reexamined to identify and extract suitable TS data, thereby facilitating an increased understanding of TS relationships for use in these surveys. However, valid *in situ* TS measurements require specific conditions (Ona, 1999), and only a small fraction of the available data is likely to be suitable for this type of analysis. Care must be taken in this process to identify and isolate valid individual targets, collect a large enough sample size, and verify the species and length composition of the scatterers (Ona, 1999; McQuinn and Winger, 2003). Typically, the selection of suitable individual targets using these criteria is performed manually (Foote, 1991; Traynor, 1996) and may be subjective (i.e. the included observations and results may change between analysts). Analysis is time-consuming, even for small datasets.

Here we describe an automated method applying a suite of published filtering methods and collection event-level criteria to existing AT survey data to objectively identify situations where TS observations can be used with confidence. The method was developed and applied to walleye pollock (*Gadus chalcogrammus*; hereafter referred to as pollock), a commercially important species subject to AT surveys in Alaska (Ianelli *et al.*, 2020). The practical goal of this work was to evaluate and confirm the validity of the length-to-TS relationship currently applied in these surveys. Abundance estimates of pollock from AT surveys in these regions are based on the length-to-TS relationship established in Foote and Traynor (1988) and confirmed in Traynor (1996):

$$TS = 20 \cdot \log_{10} L - 66.0, \quad (1)$$

where L is pollock fork length in centimetres. As is the case in many *in situ* experiments, this TS relationship was derived from a small ($n = 16$) number of paired trawl and acoustic measurements made under favourable conditions to assess individual targets. Differences in conditions between the collection of TS measurements and the survey to which they are applied remain a potential source of bias that is challenging to quantify. In the case of pollock, TS observations were collected while anchored (i.e. no vessel movement; Foote and Traynor, 1988) or at low vessel speeds and generally at night (Traynor, 1996) since the fish tend to be less densely aggregated than during the daytime. In contrast, pollock AT surveys are conducted at vessel speeds of up to 5–6 m s^{-1}, typically during the daytime when pollock are often more densely aggregated. Another example is that TS measurements collected from pollock that were not in spawning condition (Traynor, 1996) are routinely applied in surveys of spawning aggregations (McCarthy *et al.*, 2022). We apply a new method to automatically sift through a large existing AT survey data set with the goal of improving the length-to-TS relationship of pollock.

Methods

Approach

This analysis aimed to develop an unsupervised procedure to objectively screen a large set of combined echosounder and trawl data near trawl locations during AT surveys in order to select suitable TS estimates. Measurements were evaluated based on trawl catch, filters on volume backscatter, individual targets, and final conditions. The approach allows for the objective selection of final candidate TS datasets consisting of high-confidence targets, similar to targets collected following a more traditional manual, subjective process. The steps described below in sections a–c are shown in Figures 1a–c with corresponding letters. The primary parameters used in the analysis are shown in Table 1. An updated length-to-TS relationship was derived and compared to previous studies (Equation 1). Since these methods produced a large sample size from a diverse set of sampling environments, potential effects on TS were investigated.

A. Data selection and extraction

A total of 626 sets of data comprised of acoustic observations, hereafter referred to as TS sets, *s*, automatically selected in close proximity to trawl locations spanning 30 AT surveys from 2007 to 2019, were processed to extract TS measurements of pollock. Acoustic backscatter measurements were collected on the NOAA ship *Oscar Dyson* using a Simrad split-beam EK60 echosounder operating at 18, 38, 70, 120, and 200 kHz (see De Robertis *et al.*, 2019 for details). Standard sphere calibration procedures (Foote, 1987; Demer *et al.*, 2015) were performed to determine integration gain and beam angle parameters at the beginning and end of each survey and then averaged for use in post-processing. Midwater trawls targeting acoustically observed fish aggregations were conducted with an Aleutian Wing Trawl 30/20 (NET Systems, Inc.), which has a headrope and footrope length of 81.7 m. The mesh sizes taper from 325.1 cm in the forward section of the net to 8.9 cm in the codend, which was fitted with a 12 mm liner. Each trawl catch was separated by species, and individuals were weighed and measured to identify species and size composition. Random length (~350), weight, and maturity measurements (~50) on individual pollock were collected from each trawl.

Candidate TS sets were initially screened based on proximity to trawls with catch primarily composed of pollock, so that single acoustic targets were likely to be from pollock. Acoustic data that were in the spatial and temporal vicinity of trawls with catches dominated by pollock (>95% pollock by number) were identified for processing to extract TS measurements. Acoustic data collected during the survey along track lines <3 h prior to and <2 km from the location when the trawl reached fishing depth (fishing start, FS) and while the vessel was moving >4 m s^{-1}, which represents normal survey speed, were selected for analysis. The length of the analysis regions varied since the amount of data available along the survey track lines within the time and space ranges was unique to each set. These data were considered as they were collected during an initial pass over the fish aggregations during typical survey operations prior to trawling.

The average depth of the trawl headrope was computed for each selected trawl between FS and the hauling back of the trawl (HB, indicating the end of trawling target fish). The footrope depth was assumed to be 25 m deeper, based on the typical net opening. Acoustic data from 5 m above the headrope to 5 m below the nominal footrope depth (i.e. 35 m total) were included in further analyses. In these surveys, pollock are rarely in the upper 20 m, so data <20 m were excluded from further analysis. Backscatter within 5 m of the sounder-detected bottom, where fish species are more diverse (Lauffenburger *et al.*, 2017), was also excluded. Data in partial cells (not full 10 m by 10 pings) were removed from further analysis.

Single target detections within the designated location, depth, and time ranges were automatically processed (i.e. no user input due to the large volume of data) using Echoview's

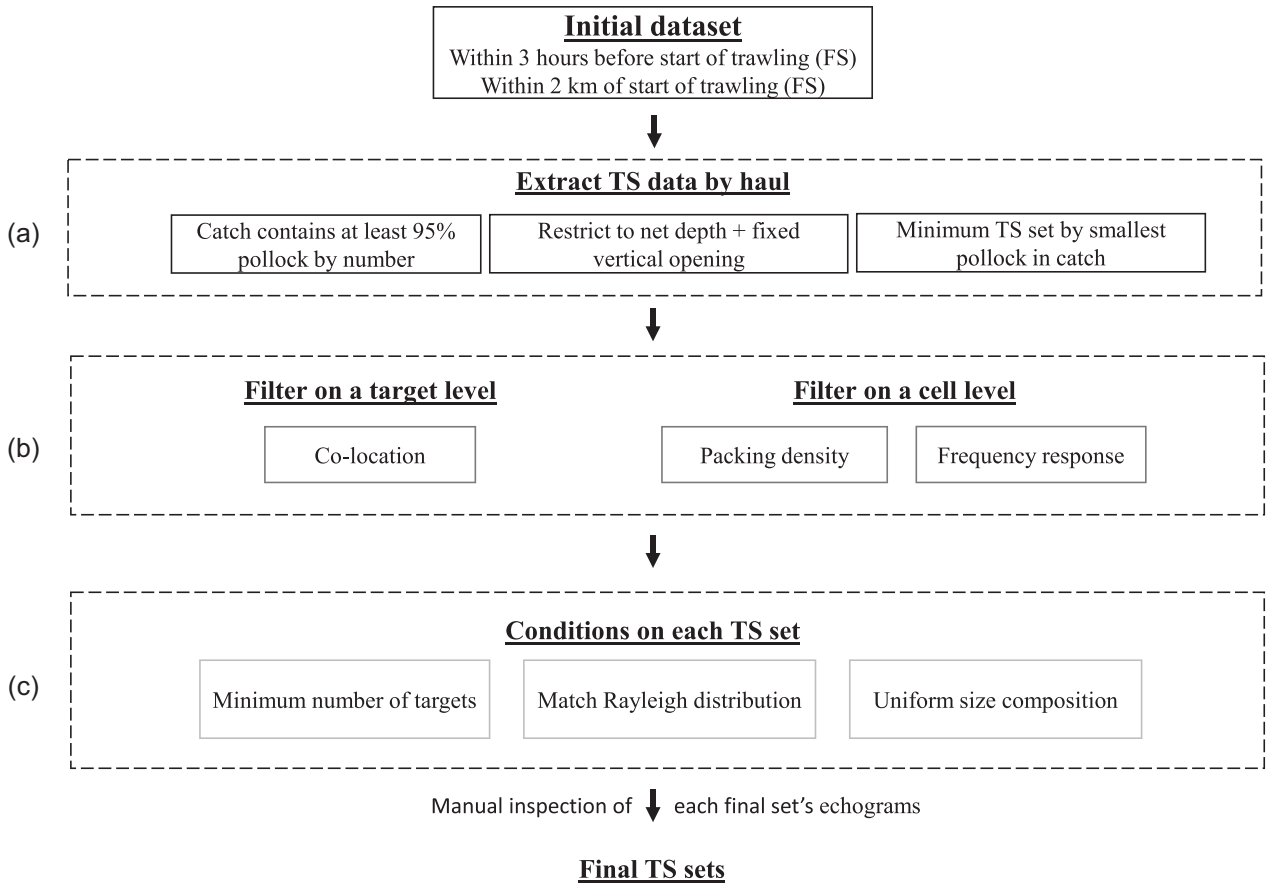

Figure 1. Diagram of processing flow for analysis, displaying (a) the extraction of TS data, (b) filtering on targets and cell level, (c) final set quality control conditions, and manual inspection of each set's final echograms. Together, these factors determine the final data used to estimate TS.

Table 1. Parameters used for data processing and thresholds applied for filtering.

Quantity	Value/Threshold
Percent pollock retained in catch	> 95%
Vertical range for target detection around trawl depth	35 m
Time range from trawling	< 3 h
Distance range from trawling	< 2 km
Minimum vessel speed	> 4 m s^{-1}
Deviation in angle for colocation	< 1.5°
Deviation in range for colocation	< 0.5 m
Acoustic data cell resolution	10 pings × 10 m
Cell resolution for packing density	100 pings × 10 m
N_v (packing density)	< 0.04
Cell resolution for frequency response	10 pings × 10 m
Z_{38-18} (two frequency response)	< 2
$\bar{Z}$ (mean frequency response)	< 2
N_s^{filt} (number of targets retained)	> 75
KS test statistic (for Rayleigh distribution)	< 0.25

(version 10.0.298, Echoview Software Pty Ltd) automation functionality (Figure 2). The single target detection algorithm for split-beam echosounders, method 2, was used with the default parameters: pulse determination level of 6 dB, minimum normalized pulse length of 0.7, maximum normalized pulse length of 1.5, maximum beam compensation of 4.0 dB re 1 m^2, and maximum standard deviation of major and minor axes angles of 0.6°. The detection parameters were chosen to be broad enough to accept many targets rather than bias the TS high from the rejection of weaker targets (Soule *et al.*, 1997).

In order to remove noise and weak non-pollock targets while retaining expected pollock targets, a minimum TS threshold for export was calculated as 20 dB re 1 m^2 lower than the expected TS of the smallest pollock in the trawl catch, L_{min}, following Equation 1. The value of 20 dB re 1 m^2 below the expected mean TS was selected as this corresponds to more than the lower bound of observed TS in previous observations (Traynor, 1996; Gauthier and Horne, 2004). The minimum thresholds used in exporting TSs ranged from -65.8 dB re 1 m^2 to -52.2 dB re 1 m^2. Each target's TS measured at

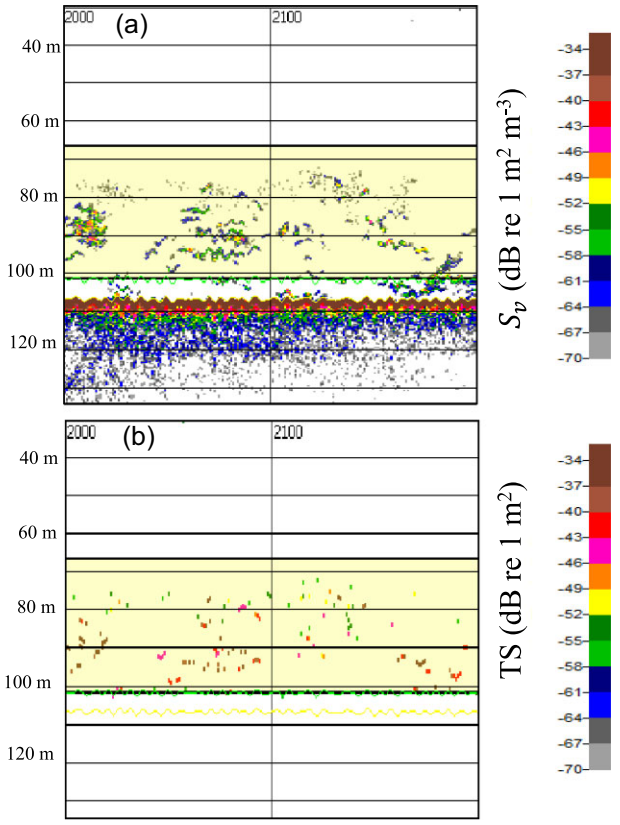

Figure 2. An example echogram of data used for single target detection with (a) raw fish backscatter (S_v, dB re 1 m ^{2} m $^{-3}$) and (b) initial single targets detected using Echoview's single target detection algorithm for split-beam echosounders, method 2 (see method text for parameter details, TS, dB re 1 m ^{2}). Vertical black lines denote a horizontal separation of 100 pings, and horizontal black lines denote a separation of 10 m. The yellow region highlights the section of the data selected based on trawl headrope depth (see methods text for data selection parameters).

38 kHz was adjusted to compensate for the over-amplification of low-power signals (<-90 dB re 1 W) by EK60 echosounders based on measurements of amplifier linearity of the specific echosounder used in this study (De Robertis *et al.*, 2019, their Figure 8). This correction only had a small effect on TS due to the relatively short ranges and strong scattering from pollock, with the effect on mean TS in a survey averaging -0.26 dB re 1 m^2.

Individual target-strength measurements, compensated within Echoview software for the horizontal position detected in the beam, were exported, and the mean volume backscatter, s_V (m^{-1}), values in these regions were exported in 10 ping by 10 m bins, hereafter referred to as cells (see Figure 2 with 100 ping separation for comparison). Target positions (range and two orthogonal off-axis angles) were computed for the 18 and 38 kHz frequencies (Ona, 1999). This initial extraction of 38 kHz targets generated 604199 TS observations at 38 kHz and 751409 targets at 18 kHz from 626 TS sets.

A lower bound of the signal-to-noise ratio was estimated from the data by converting each TS (uncompensated for horizontal position detected in the beam) to power and comparing to the highest historical passive noise measurements from the *Oscar Dyson* (Supplementary Figure S1). Since pollock targets in the data set were well above the background noise (>10 dB SNR for final targets from 0 to 125 m, see below for the final target selection process), no additional filters or compensation for signal-to-noise ratios were applied.

B. Filters applied

Colocation

Valid targets are likely to be detected in the overlapping portion of multiple acoustic beams, while artefacts and spurious noise are unlikely to occur simultaneously at multiple frequencies. Thus, the multifrequency method of Demer *et al.* (1999) was used to identify and exclude targets that were not simultaneously detected in the same location at multiple frequencies. The relative position of the transducers (38 kHz is inferred to be 0.5 m ahead of and 0.1 m to the right of the 18 kHz) was computed from the from the measurements of a 38.1 mm tungsten-carbide calibration sphere moved through both beams during the sphere calibration in 2016. These estimates were consistent with the physical separation of the transducers (38 kHz is 0.6 m in front of and in line with the 18 kHz). For each target, the position in the 18 kHz transducer was translated to the reference frame of the 38 kHz following (Demer *et al.* 1999). The absolute difference in horizontal angle and the difference in range were computed for each target. Targets were retained in this step if they were detected at both 18 and 38 kHz within 1.5 degrees of each other in alongship and athwartship angles and 0.1 m in range, as recommended by Demer *et al.* (1999).

Packing density

In cases where fish are densely aggregated, target detections can contain echoes from multiple individuals. To reduce the impact of this potential bias, TS measurements from areas with high fish densities were excluded following the method of Sawada *et al.* (1993). To reliably isolate and measure from individual pollock echoes, the density of fish was first examined. The expected number of fish in an observation volume, N_v, was estimated following (Sawada *et al.* 1993):

$$N_v = \frac{1}{2} c\tau\varphi r^2 \frac{s_V}{\widehat{\sigma_{bs}}}, \tag{2}$$

where c is sound speed (m/s), τ is the effective pulse length (s), φ is the equivalent beam angle (steradians), r is range (m), and s_V is the mean volume backscatter coefficient (m^{-1}) within 10 consecutive cells (i.e. 100 ping by 10 m regions). $\widehat{\sigma_{bs}}$ is an estimate of the backscattering cross-section for the average pollock in the trawl computed using the relationship from Equation 1, converted to linear units ($\sigma_{bs,L} = 10^{TS_L/10}$), and weighted by the proportion of pollock at length, P_L, in the trawl,

$$\widehat{\sigma_{bs}} = \sum\nolimits_L \left[\sigma_{bs,L} \cdot P_L\right]. \tag{3}$$

Targets in regions where N_v <0.04 (the same spatial scale and threshold recommended in Sawada *et al.*, 1993) were considered for further processing.

Frequency response

It is possible that the observed single targets were from small species that were poorly retained in the trawl catch. We thus excluded targets with a frequency response that was unlikely

to be from pollock. To assess whether the backscatter had a frequency response consistent with pollock, we applied the method described in De Robertis *et al.* (2010) within each 10 ping by 10 m cell. The normal deviate relative to the expectation for pollock in previous measurements, Z, was computed for the observed frequency response ($\Delta S_k = 10 \cdot \log_{10}[s_V(f)] - 10 \cdot \log_{10}[s_V(38)]$) observed at each pair-wise frequency combination ($k = f\text{-}38$) relative to 38 kHz,

$$Z_k = \frac{\Delta S_k - \mu_k}{\sigma_k}, \tag{4}$$

where μ_k and σ_k are the mean and standard deviation of the expected frequency response established in De Robertis *et al.* (2010). The mean of the absolute values of normal deviates at all frequency combinations, $\bar{Z}$, was computed. Only targets within cells where $\bar{Z} < 2$ (De Robertis *et al.*, 2010) and $Z_{38-18} < 2$ were further considered for final processing.

C. Conditions on TS sets

The 433 sets of TS observations (78328 targets) remaining after data selection and filtering, were subject to three final conditions (see Figure 1c) to ensure the quality of the final data. First, sets with <75 targets remaining after filtering, N_s^{filt}, were excluded from further processing to ensure that there were enough targets for a representative average.

To ensure that the distribution of TS measurements was likely to be representative of the size distribution of pollock in the catch, we verified that the TS distribution was consistent with the expectation of echo amplitudes with a Rayleigh distribution MacLennan and Menz (1996; Equations 5–8). The length distribution was converted to a TS distribution using a Rayleigh scattering assumption, following the methods in (MacLennan and Menz 1996). The measured TS cumulative probability distribution was compared with the computed TS distribution by calculating the Kolmogorov–Smirnov statistic iterating through intercept values of b_o, in one dB re 1 m^2 increments from -76 to -56 with a constant slope (20). Set distributions with a KS-statistic <0.25 for any b_o were retained for further analysis.

To ensure that TS measurements were associated with representative and uniform pollock lengths, we implemented a final condition on the TS sets. The variance of length distributions of walleye pollock from trawl catches can range greatly. Using trawls with a wide length distribution or with multiple length modes may result in an average length that is not representative of a majority of the individuals (e.g. if the distribution is multimodal or very broad). In addition, size distribution is more likely to be biassed by trawl selectivity, particularly when length distributions are broad and include juvenile fish (Williams *et al.*, 2011). In order to provide more confidence that the TS measurements were associated with representative pollock lengths of a single mode, only those sets with trawls containing a standard deviation of the lengths <6 cm were considered uniform in length content and used in further analysis. The selection of a 6 cm standard deviation threshold reliably separated the length modes associated with pollock at year 1, year 2, and year 3 + classes (Jones *et al.*, 2019).

The 144 sets that passed all selection criteria described above (Figure 1) were used as final candidate TS sets in the analysis. As a final measure of quality control, each set's echogram of S_V (volume backscattering strength: $10 \cdot \log_{10} s_v$) and single target for the exported region were visually inspected if any additional artefacts were present. This was the only manual step in the analysis and took <1 h to review. Based on this step, two sets with acoustic interference (noise) were identified and removed from the final dataset. A final collection of 142 sets containing 51968 TS observations spanning the years 2007–2019, with the exception of 2009 and 2010 (11 years), was used in the analysis.

Model fitting and selection

For each selected TS set that passed all conditions after filtering, a mean TS, TS_s, was computed by averaging all valid targets' backscattering cross-sections, $\overline{\sigma_{bs,s}}$, and then converting to log scale ($TS_s = 10 \cdot \log_{10}(\overline{\sigma_{bs,s}})$). The mean length, L_s, of pollock in the associated trawl was then computed. A linear regression, following the form of Equation 1, was fit:

$$TS_s = m \cdot \log_{10} L_s + b. \tag{5}$$

Confirming a fixed-slope base model

Additionally, a linear regression, holding the slope, m, constant at 20 dB re 1 m^2, was fit:

$$TS_s = 20 \cdot \log_{10} L_s + b_f. \tag{6}$$

Using a constant slope of 20 dB assumes that σ_{bs} increases with the cross-sectional area of the fish, which scales with L^2. Generalized linear models (GLM) were fit with the R function "GLM" (version 4.0.4, R Core Team, 2021).

To compare the predictive power and assess the practical performance of these two models, leave-one-out cross-validation (LOOCV) was performed for each model. Each set was removed and both models were fit without the withheld observation, and the squared difference between the actual, TS_s and predicted, TS_s^{pred}TS of the withheld observation was computed. The root mean square error (RMSE) was computed across all the predicted values using the total number of sets N:

$$RMSE = \sqrt{\sum_s (TS_s - TS_s^{pred})^2 / N}. \tag{7}$$

The RMSE for the fixed slope model (Equation 6) was marginally less (1.62 dB re 1 m^2) than the free slope model (1.64 dB re 1 m^2, Table 2A–B), which indicated that allowing the model to fit a slope did not add predictive power. Therefore, Equation 6 with a fixed slope was treated as the base model. Rearranging Equation 6 with a constant slope of 20, the y-intercept becomes the non-dimensional reduced TS (TS normalized by surface area), RTS (dB re 1 m^2 m^{-2}), which allows convenient comparison of observations across a range of lengths. Starting with rearranging Equation 6:

$$b_{f,s} = TS_s - 10 \cdot \log_{10} {L_s}^2. \tag{8}$$

This can be expressed in linear units:

$$b_{f,s} = 10 \cdot \log_{10} \overline{\sigma_{bs,s}} - 10 \cdot \log_{10} {L_s}^2. \tag{9}$$

And expressed as the reduced TS for each set:

$$RTS = 10 \cdot \log_{10} \left({\overline{\sigma_{bs,s}}}/{{L_s}^2} \right). \tag{10}$$

The average RTS over all sets s, an estimate of the average TS of pollock, regardless of size, is computed for the mean as:

$$\overline{RTS} = b_f = \left({1}/{N}\right) \cdot \sum_s RTS. \tag{11}$$

Table 2. Model descriptions and parameter values of sample models used in fitting the average length to the average TS measurements by set with final filtered data ($N = 142$).

Type		Model	Description	Parameter	Estimate	Std. error	ΔAICc	LOOCV RMSE
GLM								
	A	$TS_s = m \cdot \log_{10} L_s + b$	Two parameter model, Equation 5	m b	18.3 −63.4	1.5 2.37	0	1.64
	B	$TS_s = 20 \cdot \log_{10} L_s + b_f$	One parameter model with fixed slope, Equation 6	b_f	−66.0	0.14	−1	1.62
GAM (Generalized additive model)	C	$TS_s = 20 \cdot \log_{10} L_s + s(T_s) + s(D_s) + s(YR_s) + s(TD_s) + s(M_s) + GR_s + S_s$	Full GAM fit to all parameters, Equation 15	-	-	-	−19	1.62
	D	$TS_s = 20 \cdot \log_{10} L_s + s(T_s) + s(D_s) + s(YR_s) + s(TD_s) + S_s$	Intermediate GAM fit after removing region and maturity based on AICc	-	-	-	−23	1.62
	E	$TS_s = 20 \cdot \log_{10} L_s + s(T_s) + s(D_s) + S_s$	Final GAM fit, including significant predictors *in situ* temperature, depth, and season	-	-	-	−26	1.54
GLM (environmental effects)	F	$TS_s = 20 \cdot \log_{10} L_s + m_D \cdot D_s + m_T \cdot T_s + S_s + b_a$	GLM for significant predictors, with a linear depth effect from the surface to 126 m, and the effect at deeper depths held constant ($D_s = 126$)	m_T m_D S_w b_a	−0.14 0.03 −0.95 −67.7	0.06 0.006 0.43 0.56	−27	1.49
	G	$TS_s = 20 \cdot \log_{10} L_s + m_D \cdot D_s + b_D$	GLM with only the depth effect from F	m_D b_D	0.03 −68.4	0.006 0.54	−18	1.53
	H	$TS_s = 20 \cdot \log_{10} L_s + m_T \cdot T_s + b_T$	GLM with only the temperature effect from F	m_T b_T	−0.16 −65.4	0.06 0.27	−6	1.60
	I	$TS_s = 20 \cdot \log_{10} L_s + S_s + b_s$	GLM with only a season effect from F	S_w b_s	−1.2 −65.9	0.46 0.14	−6	1.60

RMSE from LOOCV and the AICc change relative to model A (ΔAICc) for model selection are shown for each model fit. Standard errors are included for each parameter for the linear fits. Grey shading delineates the base linear model, the final GAM model, and the summary GLM model with environmental effects. The parameter estimate for the season effect is shown for winter ($S_s = S_w$) in F and I. For summer, the season effect is 0 (i.e. $S_s = S_{sum} = 0$).

Sensitivity analysis

Final data selected for model fitting depended on the choice of filter and set condition values (see Table 1), so it was important to assess the sensitivity of our model estimates to changes in these thresholds. To evaluate the sensitivity of the pollock TS estimates on each filter or condition, a one-at-a-time sensitivity analysis was performed. Cycling through each filter or condition, the selected threshold V was varied by the following multiples of the nominal value (Table 1; None, $\frac{1}{4} \cdot V$, $\frac{1}{2} \cdot V$, V, $2 \cdot V$, $4 \cdot V$), with all other terms held at their nominal value. None was defined as not applying V at all, so that the influence of removing that filter or condition could be assessed. For each filter and condition in the set, the values of RTS were derived for each threshold option listed above.

Predictors of TS

The final TS sets spanned many years and conditions, including different depths, *in situ* water temperatures, seasons, pollock maturities, geographical regions, and time of day. We evaluated the potential influence of these factors on variations in TS. Mean depths of all filtered targets by the TS set, D_s were computed to assess a depth effect. Mean sea temperatures (°C), T_s, associated with each TS set were computed by averaging the temperature measured with a Sea-Bird temperature-depth probe (SBE-39, Sea-Bird Scientific) mounted on the headrope of the trawl between FS and HB. Sets were labelled with the year, YR_s, the time of day estimated from the sun angle, TD_s, at FS to assess diel changes and assigned a season, S_s, as either winter (February–March) or summer (June–August). The % of pollock >30 cm that were classified as reproductively mature, M_s, based on morphological examination (Williams, 2007) was computed. In a small number of cases ($n = 6$), maturity data were not collected in the trawl sample, and the proportion of mature adults from the nearest trawl during the same survey was applied. Data were assigned a geographic region, GR_s (i.e. eastern Bering Sea, EBS, or Gulf of Alaska, GOA). To identify any collinearity between the potential predictors, Pearson correlation coefficients were computed between the non-categorical effects.

Model selection

The environmental and physiological effects potentially influencing pollock TS were explored using GAMs were fit using the R package mgcv (Wood and Augustin 2002, version 1.8.33). The set averaged filtered observations, TS_s, were fit with potential predictors expanding the base fixed slope model in Equation 6. The GAMs assume that each predictor is an additive factor or a smoothed function implemented as penalized regression splines. Given that pollock TS scaling by length was found to be consistent with L^2, the mean length, L_s, was held as an ordinary log-linear parametric term with a fixed slope of 20. Categorical covariates season and geographic region were treated as factors. The full model's form was:

$$TS_s = 20 \cdot \log_{10} L_s + s(T_s) + s(D_s) + s(YR_s) + s(TD_s) + s(M_s) + GR_s + S_s + \varepsilon, \quad (12)$$

where ε was assumed to be an independently and identically distributed error term. The number of splines used as basis functions for each smooth term was limited to a maximum of $k = 2$, since any highly non-linear relationship could not be easily explained based on current theory.

Backwards variable selection was used to determine the relative importance of each predictor mentioned above using the second-order Akaike Information Criterion corrected for finite sample sizes (AIC_c; Burnham and Anderson, 2004). The full model was fit, and then one covariate at a time was dropped based on the lowest AIC_c score. Elimination of predictors continued until the model AIC_c no longer improved. Forward variable selection produced the same result. Plots of residual data were examined to confirm that the error distribution was satisfied as assumed.

Derivation of new TS GLM model

To facilitate practical application during AT surveys, it is desirable to parameterize the depth, temperature, and season effect identified in the GAM analysis in a simplified form. Thus, the TS GLM (Equation 6) was modified to account for a nonlinear depth effect and the environmental predictors identified in the GAM analysis that best explained variations in TS. The model was developed to parameterize the depth, temperature, and season effect for practical application. The basic form of the final model was:

$$TS_s = 20 \cdot \log_{10} L_s + m_D \cdot D_s + m_T \cdot T_s + S_s + b_a. \quad (13)$$

Given that the depth effect on TS in the GAM appeared linear for shallower fish and likely remained constant in deeper waters (see results, Figure 7a), a hybrid form for the depth effect was developed. A linear effect was assumed between the surface and a threshold depth, D_x. No further influence of depth on TS was assumed to be present below that threshold (i.e. $m_D = 0$, where $D_s \geq D_x$). This forced TS to remain constant with respect to depth for all depths greater than the threshold. An optimizer (R package optim) was used to minimize the sum of the squares of the simplified model with length and depth ($TS_s = 20 \cdot \log_{10} L_s + m_D \cdot D_x$), allowing the unknown depth threshold, D_x, to vary. The full model (Equation 13) was then fit using the estimated depth threshold (D_x= 126 m). Three alternative GLM models were fit, each with a single predictor from the final set of significant factors (Table 2 G–I).

Results

In situ TS observations

The final TS estimates from the final candidates with filters and set-level conditions applied ($n = 142$) exhibited substantially less variability than those based on the raw ($n = 626$) or filtered targets ($n = 433$; Figure 3). Linear regressions fit to the final dataset with a slope fixed to 20 (Equation 6) and a free slope (two-parameter, intercept and slope, Equation 5) produced predictions of TS (Figure 3, Table 2). The confidence intervals of the intercepts of the free slope model (-63.64 dB re 1 m^2, 95% CI = [-68.1, -58.7]) and the fixed slope model (-66.04 dB re 1 m^2, 95% CI = [-66.3, -65.8]) overlapped, indicating that they are not statistically different. The slope parameter estimate of the free slope model (18.3) was also not significantly different from 20 (95% CI = [15.4, 21.3]). Additionally, the LOOCV analysis did not show a notable difference in the RMSE between the models (1.62 dB for fixed slope vs. 1.64 dB for free slope; Table 2 A–B). As noted in the previous section, this indicated that the addition of a slope parameter is slightly less predictive when estimating out-of-sample data. Thus, a model with a fixed slope of 20 was used in further analyses.

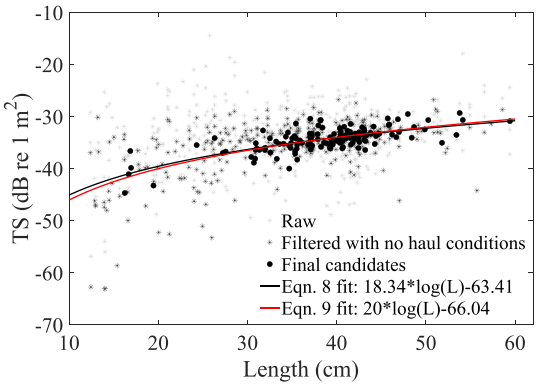

Figure 3. Average TS measurements by set for raw data without any treatment (i.e. without any filtering, light grey stars Figure 1a), filtered data with no set conditions (i.e. haul, target, and cell-level criteria applied, see Figure 1b, dark grey stars), and final sets selected for modelling (i.e. all criteria applied, see Figure 1c, black circles). Two linear regression fits are shown for $log_{10}L$ as the independent variable and TS as the dependent variable: Models were fit to the slope and intercept (black line) and to just an intercept with the slope fixed at 20 (red line).

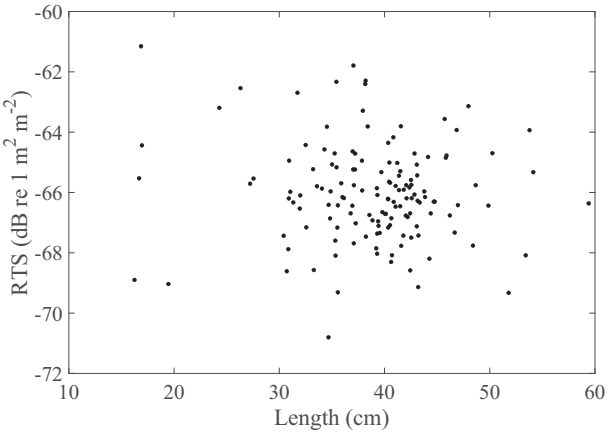

Figure 4. Reduced target strength (RTS, dB re 1 m ^{2} m $^{-2}$) as a function of average pollock length. RTS represents the TS normalized to length^2 (see Equations 8–11 in the text for details).

Sensitivity analysis

The average RTS in each set was not significantly correlated with mean pollock length (Figure 4, r = -0.09), and individual observations ranged from -70.8 to -61.2 dB re 1 m^2 m^{-2} with a median of -66.2 dB re 1 m^2 m^{-2}. The sensitivity analysis indicated that RTS was robust to moderate changes in the choice of parameters used for processing (Figure 5). Changing the filter parameters (Figure 5a–c) had a relatively small impact on RTS when a threshold was applied (i.e. all cases but "None"), causing differences in the median or mean values of <1 dB over changes of ±50% in parameter thresholds. When filters were applied (not "None"), 95% confidence intervals overlapped those of the chosen value (notches, Figure 5). The greatest changes in RTS resulted when a given filter was not applied. The change in the median of RTS_s values from filters (Figure 5a–c) was greatest for the packing density filter (Figure 5, with 2.0 dB re 1 m^2 m^{-2} higher in the "None" case compared to the most restrictive case (0.02). RTS showed relatively small changes based on the threshold selection in each of the set conditions (Figure 5d–f), with the KS-statistic having the largest change in distribution from the most to least restrictive condition thresholds, mainly due to a small sample size in the most restrictive case. Median RTS was least sensitive to the minimum number of targets, showing only minor effects on the mean RTS (Figure 5d) across all tested thresholds.

Explanatory variables

RTS summarized by depth, region, season, and temperature shows variation with these factors (Figure 6), suggesting that each of these variables may influence pollock TS. The median RTS was highest for the cool temperature (<4°C) group (-65.8 dB re 1 m^2 m^{-2}) and the lowest in the winter (–67.4 dB re 1 m^2 m^{-2}). The predictor with the largest difference in median was season, where the change in median between summer and winter was 1.3 dB re 1 m^2 m^{-2}. All categories except maturity exhibited a difference >0.5 dB re 1 m^2 m^{-2} in median and mean RTS between their subcategories (e.g. shallow vs. deep, winter vs. summer, etc.), indicating that depth, season, temperature, and region may influence pollock TS.

GAM models

Three environmental covariates, depth, season, and temperature, were retained in the GAM after model selection (Table 2), indicating that accounting for these variables can improve estimates of pollock TS. Mean depth was the most significant factor in the GAM model fit from the forward variable selection (Figure 7a). The depth effect showed a close to linear increase in TS at a rate of about 0.2 dB re 1 m^2/10 m from depths 40.5 to 125 m, with higher uncertainty and few observations below that depth. Season was the second-most significant contributor to the model, with an intercept of -66.0 dB re 1 m^2 in summer and an intercept of -67.0 dB re 1 m^2 in winter. The last covariate retained in the model was the *in situ* trawling temperature, indicating a decrease of about 1 dB re 1 m^2 from cold (-0.9°C) to warm temperatures (8.9°C; Figure 7b). Examination of residual plots and the Q-Q relationship for the final GAM model indicated that the residuals were largely homoscedastic and normally distributed (Supplementary Figure S2), consistent with the initial model assumptions.

Simplified models

The final GLM fit for TS produced results (Table 2F) provided a good approximation of the final GAM model. Using a linear fit to temperature and a linear depth effect down to a computed depth (D_x= 126 m) with a fixed depth effect below that threshold, produced a model with a LOOCV RMSE of 1.49 dB re 1 m^2. This demonstrated that the new model better predicted out-of-sample TS data than the GAM (compare Table 2E and F) and can be used as a practical replacement for the GAM. Each significant predictor was fit alone in three separate models (Table 2G–I) to provide values for application in cases when not all environmental indicators have been collected or are available, although predictive power is lost in these models.

Impact of a new TS on pollock abundance estimates

We evaluated the impacts of altering the TS relationship on pollock surveys in Alaska by re-computing abundance using the final TS relationship, including depth, temperature, and season for the summer and winter AT surveys in the GOA

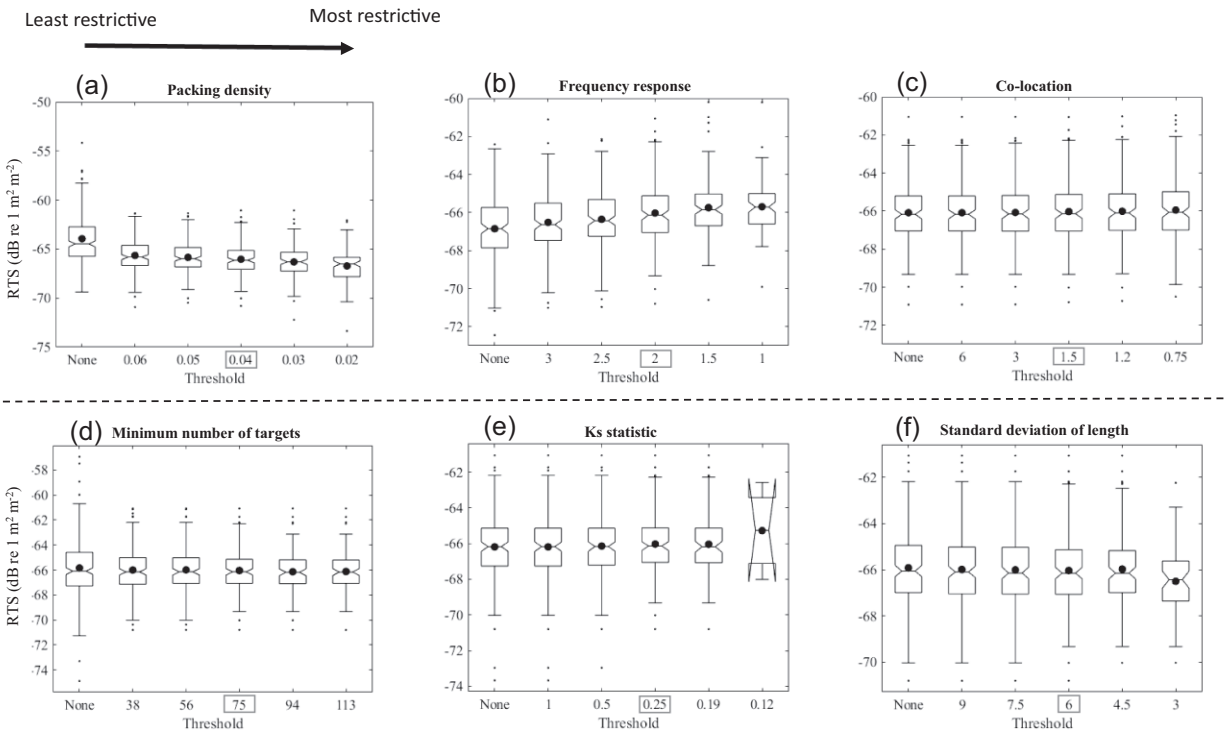

Figure 5. Sensitivity analysis showing the impact of varying thresholds (Figure 1b–c) of individual criteria used in the analysis of RTS with all other criteria set at their nominal values (boxed on the x-axis label). The distribution of RTS values is shown for each filter (top row) as (a) packing density, (b) frequency response, (c) colocation, and set conditions (bottom row) as (d) minimum number of targets, (e) KS-statistic, and (f) standard deviation of length. "None" indicates that the filter was not applied. All figures show the least restrictive thresholds on the left and the most restrictive thresholds on the right. The horizontal line within each box represents the median value in that distribution, and the black dot within each box represents the mean value. The box contains the interquartile range, the whiskers extend to the top and bottom quartiles of the data and notches in each box show the 95% confidence intervals (subplot e has confidence intervals that exceed the interquartile range for a value of 0.12). Limits on the y-axis vary in each subplot due to variable ranges between the filters and conditions. For packing density, a single point was omitted in the "None" category at -32.7 dB.

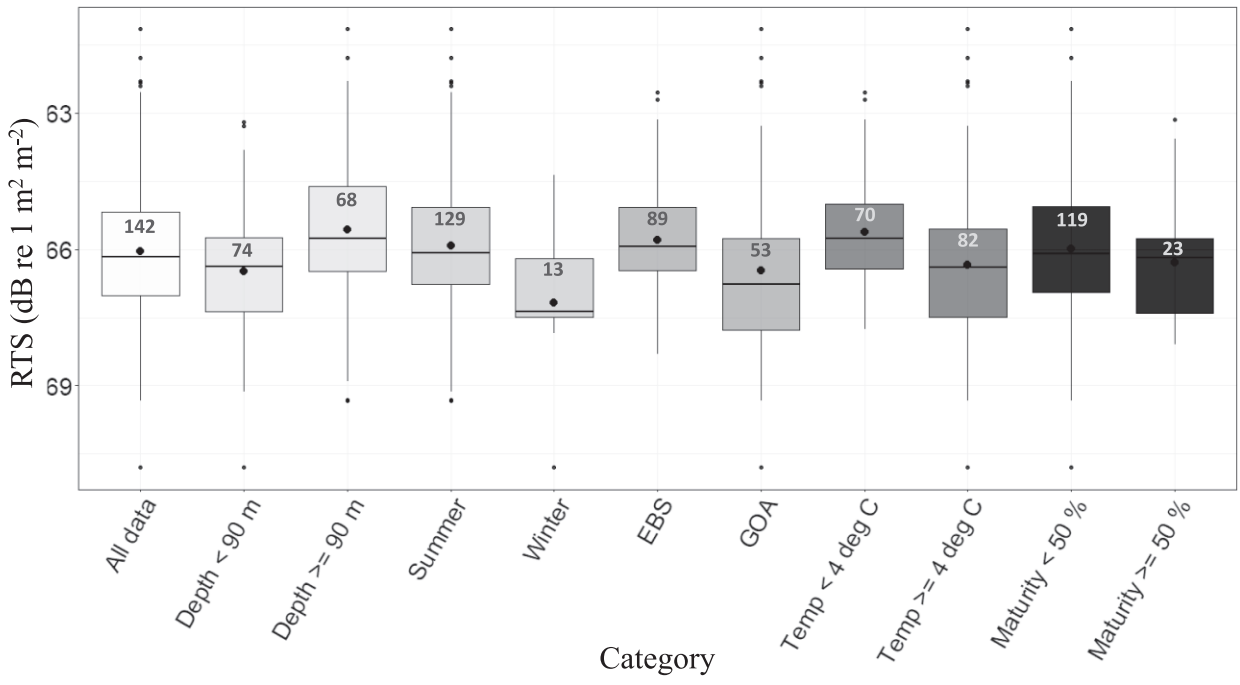

Figure 6. Final reduced target strength (RTS, dB re 1 m ^{2} m $^{-2}$) estimates for all sets. Data have been grouped (by colour) into all data, shallow (<90 m, mean of all depths), deep (≥90 m), summer, winter, EBS (eastern Bering Sea), GOA (Gulf of Alaska), cool temperatures (<4°C, mean of all temperatures), warm temperatures (≥4°C), low ratio of mature fish in the catch (<50%), and high ratio of mature fish (≥50%). The horizontal line within each box represents the median value in that distribution, and the black dot within each box represents the mean value. The number in each box plot is the sample size for that category. The box contains the interquartile range, and the whiskers extend to the top and bottom quartiles of the data.

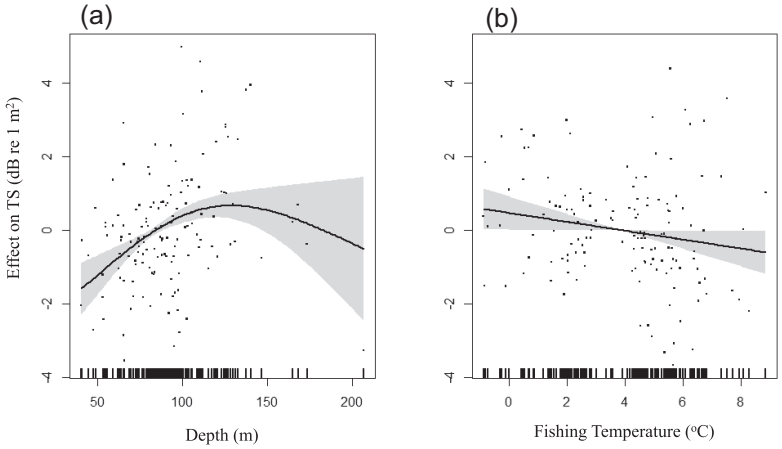

Figure 7. GAM fits on TS showing the partial effect of (a) depth (m) and (b) temperature (°C). The black circles are the partial residuals from the model for each predictor, and the black lines are the smoothed functions of each term. The shaded regions represent the 95% confidence interval around each fit.

and EBS. Pollock abundance estimates were recomputed with the new TS model (Table 2F) and compared to historic estimates based on the base model (Equation 1). Applying the GLM form of the TS model with all significant environmental covariates included (Table 2F) to estimates of pollock numerical abundance from 2007 to present yielded changes that spanned from -16.3 to + 21.0% relative to the historic estimates using the base model in Equation 1 (Supplementary Table S1). The average changes were -8.5% in the EBS, -3.4% in the winter Shelikof survey, and -5.7% in the summer GOA survey.

Discussion

New automated method: mining old surveys

A large volume of calibrated echosounder data can be found in past AT survey archives (Wall *et al.*, 2016). However, it is challenging to extract unbiassed targets from these data. An automated method to extract existing survey data TS measurements by use of trawl catch and a set of published filtering methods (Sawada *et al.*, 1993; MacLennan and Menz, 1996; Demer *et al.*, 1999; De Robertis *et al.*, 2010) has been demonstrated here and applied to pollock. Although the individual analytical components of this study have been established previously, we present an innovative combination of these methods to mimic the traditional manual, somewhat subjective, target selection process in an automated, objective way applied to a large data set.

Extracting TS from survey data (Rudstam *et al.*, 2009; Stevens *et al.*, 2021), if done reliably, is advantageous for computing abundance estimates of fish. Applying TS data collected during typical survey conditions (at typical vessel speed, normal hours of collection, etc.) results in a TS relationship that is representative of the fish observed during that survey. In many situations, however, it is not possible to estimate TS during survey conditions due to the aggregation of the fish. Although TS measurements collected during survey operations may incorporate potentially ship-specific vessel avoidance behaviour (De Robertis *et al.*, 2010), the survey-collected TS data are most relevant to converting survey-collected backscatter data to abundance under a specific set of survey conditions (Fleischer *et al.*, 1997). Other approaches, including measuring *in situ* TS during nighttime operations at reduced vessel speeds (Madirolas *et al.*, 2017), with a lowered echosounder (Kloser *et al.*, 1997), and *ex situ* TS measurements collected in a controlled pen or laboratory setting (Thomas *et al.*, 2002), may not capture survey conditions appropriately. Additionally, TS modelling efforts (Sawada *et al.*, 1999; Horne, 2003) have shown the effects of behaviour (orientation) and physiology on TS measurements (Ona, 1990), but it is challenging to extrapolate those results to survey-averaged conditions. For example, even though there is an understanding of how orientation influences TS (McQuinn and Winger, 2003; Hazen and Horne, 2004), the orientation of individuals during survey conditions remains poorly characterized.

The data selection process (Figure 1) yielded 51968 targets from 604199 raw targets, an acceptance rate of 8.6%. Low retention of targets was expected given the high level of contamination in the raw data due to factors such as pollock distributed in high-density schools, noise, the presence of non-pollock targets in the water column, multimodal or broad fish length distributions, and low numbers of single targets. The data filters were designed to identify and exclude these cases. Further, the sensitivity analysis of the threshold choice for each filter and set condition suggested that the final results were not highly impacted by the specific parameters used for data selection. RTS values were not highly sensitive to the choice of threshold applied to each filter and set condition, except in instances where no threshold was applied. Applying the packing density filter had the largest impact on the mean RTS, where the mean dropped 1.5 dB when changed from "None" to 0.06, the least restrictive value. This indicated that the use of a fish density filter was likely the most important step in selecting individual targets within each cell. This finding is not surprising, as trawling typically occurs on high-density aggregations (McCarthy *et al.*, 2022). Varying all the filters resulted in modest changes to the TS distribution, typically by <1 dB re 1 m^2, providing confidence that the TS estimates were not highly sensitive to the choice of processing parameters.

Pollock TS

Without including any covariates, the selection of candidate targets and sets resulted in a fixed slope length-to-TS relationship (Figure 3), remarkably similar to the one published in the past with far fewer observations and employing less sophisticated instrumentation and processing techniques (Traynor, 1996). The estimated RTS of -66.04 dB re 1 m^2 m^{-2} is consistent with the measurements of Traynor, 1996 (-66.0 dB re 1 m^2 m^{-2}) and Hazen and Horne, 2004 (modelled -67 dB re 1 m^2 m^{-2} and measured -66 dB re 1 m^2 m^{-2}). The new measurements reported here give us more confidence in the survey application of these results, which are based on a larger data set over a wide range of years and the data are more applicable (e.g. vessel was at survey speed). The method described in this paper successfully gathered suitable TS averages for pollock ranging from 17 to 60 cm in average length, with most observations corresponding to adult pollock (>30 cm). For juvenile pollock (10–30 cm, typically ages 1 and 2), the number of final candidate sets was limited, likely due to schooling behaviour in younger fish, resulting in fewer individual targets detected and thus a higher level of exclusion by the packing density filter (Sawada *et al.*, 1993). The RTS of these juveniles was more variable than that for adult pollock (Figure 4), and the model fit may not agree as well for these smaller fish (Figure 3), possibly due to differences in behavioural effects. Future work on pollock TS should focus on smaller pollock, which may exhibit a different length-to-TS relationship than adults (Abe *et al.*, 2004, RTS of -67.8 dB re 1 m^2 m^{-2} for <20 cm pollock). Despite the advantages of making TS estimates during survey conditions, other approaches such as lowered platforms transmitting broadband signals offering increased range resolution (e.g. Lavery *et al.*, 2017; Cotter *et al.*, 2021), may be required to generate larger sample sizes of reliable *in situ* TS measurements from aggregated small pollock.

Environmental effects on pollock TS

TS depends on the behaviour and physiological state of fish as well as size (Ona, 1990), but this is rarely considered for use in acoustic surveys. The models developed in this paper give further insight into how the inclusion of both behavioural and environmental effects may improve pollock TS estimates for surveys. Target depth was the most significant predictor of TS. Previous studies of diel migration in gadoids (Atlantic cod, *Gadus morhua*, and blue whiting, *Micromesistius poutassou*) have observed higher TS in shallower distributions at night compared to deeper measurements during the day, attributing the trend to differences in swimbladder inflation (Rose and Porter, 1996; Johnsen and Godø, 2007), consistent with an uncompensated reduction in swim bladder volume with Boyle's law (Hazen and Horne, 2004 their Figure 7, Mukai and Iida, 1996). However, in our case, time of day was not a significant factor in the model, suggesting that the causes of depth-dependent changes in TS are likely situation- and species-specific.

The lower TS observed near the surface in this case is likely attributable to a depth-dependent fish diving behavioural response to the approaching vessel (De Robertis and Handegard, 2013). If pollock closer to the vessel (i.e. shallow fish) are more likely to exhibit a stronger avoidance response, they would be more likely oriented vertically (head-down) compared to pollock at greater depths (De Robertis *et al.*, 2010). As fish dive, TS tends to decrease as the swim bladder subtends a smaller projected area. Modelling work for pollock has shown a 10° change in tilt angle may decrease TS by up to 3 dB (Hazen and Horne, 2004, their Figure 4), and *in situ* target tracking TS observations during trawling observed a RTS change of 6 dB in Atlantic cod with a change in 10° tilt angle (McQuinn and Winger, 2003). Rose, 2009 found a similar effect in the diel behaviour of Atlantic cod in that shallower fish had a lower TS, showing a strikingly similar depth dependence (0.05 dB/m, see Rose, 2009; Equation 2) to that determined here for pollock (0.03 dB/m, Table 2, Equations F and G). Comparison of a wind-powered autonomous vehicle and the noise-reduced research vessel used to collect the data in this survey has shown that shallowly distributed pollock (30–100 m) dive in response to the survey vessel used in this study, but that deeper (>90 m) pollock do not (De Robertis *et al.*, 2019). Thus, the observed lower TS of shallowly distributed fish is consistent with a depth-dependent avoidance reaction to the approaching ship, which becomes negligible for fish deeper in the water column (>125 m).

Temperature was the second most important predictive covariate of pollock TS, decreasing with increased temperature (Figure 7). Again, this is likely not due to changes in swim bladder volume from Boyle's law because swim bladder size is expected to increase with temperature. The effect of temperature on TS is unclear but may be linked to temperature effects on behaviour. One study showed that juvenile pollock tend to swim faster and in straighter paths in cold temperatures (Hurst, 2007). If there is indeed more variance in the direction of swimming paths during warmer temperatures for pollock, higher temperatures could result in a larger proportion of pollock at orientations deviating from normal to the echosounder, thus causing a decrease in TS.

Seasonality was the final significant predictor of TS, with a lower intercept in winter months, which is unlikely to be attributed to temperature differences; season and temperature were considered explicitly as a separate effect in our analysis and showed an increase of TS in colder temperatures. In fact, temperature differences in our data set were more strongly associated with location than with time of year. The computed Pearson correlation coefficients between temperature and latitude (-0.68) and longitude (0.80) were much higher than those between temperature and month (0.28). Another possible explanation for seasonality as a predictor of TS could be a reduction of the swim bladder volume in winter months due to the increased size of gonads in the body cavity of mature pollock during spawning (Williams, 2007). This, however, may be unlikely since maturity state, which is a better proxy for the impact of gonad shape/size on the swim bladder, was explicitly included in the initial full model but not selected. Another possible explanation for the seasonal effect could be lower TS due to swimbladder compression by increased stomach contents (Ona, 1990) in the winter months. However, the ratio of pollock stomach content to body weight tends to be lower in the winter months (Dwyer *et al.*, 1987). Further work to examine the cause of the seasonal effect of pollock TS would be valuable.

Use of a new TS relationship with all significant covariates included (Table 2F) resulted in modest changes (<9% on average, see results) in abundance of pollock relative to the historic estimates with a base model (Equation 1). Use of this new TS model will introduce behavioural and environmental effects on survey abundance estimates; for example, the largest annual changes were driven by increases in TS associ-

ated with relatively deeper pollock in colder water during the summer in the EBS (e.g. Supplementary Figure S3, subplot c, year 2008) and lower TS from relatively shallower pollock in warmer temperatures during the Shelikof winter survey (e.g. Supplementary Figure S3, subplot c, year 2016). Since there can be changes in these effects within a survey, the inclusion of one or more of these parameters likely will increase the accuracy of year-over-year abundance estimates.

Limitations

The method outlined here has specific requirements for the type of trawl and acoustic data used as input. A calibrated multifrequency split-beam acoustic system with multiple frequencies is needed to properly measure TS observations and implement these filtering methods. To successfully identify many final filtered target sets from initial raw data, trawl sites where single targets are dominated by a single species of consistent size are needed to reliably match the fish with TS measurements. Otherwise, the ability to correlate individual TS measurements with particular species in the catch is lost. In addition, fish need to be distributed relatively shallowly or within a modest range of the transducers ($<\sim$150 m below the ship-mounted echosounders in this case) so that echoes from individuals can be resolved. Finally, if the species of interest tends to aggregate into dense schools, single target detection is limited, and the packing density filter will likely remove most of the cells with fish, as very few individual targets will be valid. These requirements were largely met for the pollock data set described here; however, smaller pollock (<30 cm), which tend to school more closely (i.e. juvenile pollock aggregate more closely adult pollock, Stienessen *et al.*, 2019), were probably not as available to TS measurement by this methodology as larger pollock were. It is important to recognize that even when single targets are detectable outside of aggregations, the TS measured from individuals outside of a dense school may not represent those within the school since there could be differences in species, size composition, or behaviour within and outside schools.

Conclusions

Application of a new automated and objective method resulted in the derivation of an updated pollock TS relationship using a much larger volume of data than available from previous work (Traynor, 1996; Hazen and Horne, 2004). The resulting length-to-TS relationship with the form $20 \cdot \log_{10} L$ was very similar to the existing relationship used in routine surveys (Traynor, 1996). A new collection of GLM models (based on initial GAM results, Table 2F–I) that included covariates were developed to describe how pollock TS may be influenced by target depth, fishing temperature, and seasonality. Utilizing additional covariates for survey abundance estimates of walleye pollock should improve accuracy, especially given that the TS measurements used in this study were made under survey conditions.

The methods presented in this study should generally be applicable to acoustic surveys where large amounts of backscatter data are collected in conjunction with trawling samples dominated by a single species. Survey echosounder measurements with trawl-verified catch are likely to contain information that can be used to reduce uncertainties by better estimating *in situ* TS. Although there are many long-standing AT surveys, TS estimates made during routine survey operations have been historically underutilized due to the difficulties associated with identifying suitable observations of TS in the context of a large number of potentially biassed observations. This study indicates that useful TS measurements can be buried in existing datasets, ready to be uncovered, and with some attention to methodology, these datasets can be effectively data-mined to good effect.

Acknowledgements

We want to thank all the people who participated in the eastern Bering Sea and Gulf of Alaska acoustic-trawl surveys, as this project was contingent on the availability of these data. We also thank Cole Monnahan, David McGowan, Patrick Ressler, Sandy Parker-Stetter, and Michael Martin for reviews and discussions that improved the quality of this manuscript. The findings and conclusions in the paper are those of the author(s) and do not necessarily represent the views of the National Marine Fisheries Service, NOAA. Reference to trade names does not imply endorsement by the National Marine Fisheries Service, NOAA.

Supplementary data

Supplementary material is available at the *ICESJMS* online version of the manuscript.

Data availability

The data underlying this article will be shared on reasonable request to the corresponding author.

Author contributions

A.D.R., K.W.: conceptualization; all authors contributed to data curation, investigation and formal analysis; N.L.: writing—original draft; all authors contributed to writing—review and editing.

Conflict of interest

The authors have no conflict of interest to declare.

References

Abe, K., Sadayasu, K., Sawada, K., Ishii, K., and Takao, Y. 2004. Precise target strength measurement and morphological observation of juvenile walleye pollock (Theragra chalcogramma). In Oceans' 04 MTS/IEEE Techno-Ocean'04(IEEE Cat. No. 04CH37600) 1: 370–374. https://doi.org/10.1109/OCEANS.2004.1402945. last accessed 6 february 2023.

Burnham, K. P., and Anderson, D. R. 2004. Multimodel inference: understanding AIC and BIC in model selection. Sociological Methods & Research, 33: 261–304.

Cotter, E., Bassett, C., and Lavery, A. 2021. Comparison of mesopelagic organism abundance estimates using in situ target strength measurements and echo-counting techniques. JASA Express Letters, 1: 040801.

Dalen, J., and Bodholt, H. 1991. Deep towed vehicle for fish abundance estimation concept and testing. ICES CM, 1991/B: 13.

Demer, D. A., Berger, L., Bernasconi, M., Bethke, E., Boswell, K., Chu, D., Domokos, R. *et al.* 2015. Calibration of acoustic instruments. ICES Cooperative Research Report, 326:133.

Demer, D. A, Soule, M. A., and Hewitt, R. P. 1999. A multiple-frequency method for potentially improving the accuracy and precision of *in situ* target strength measurements. The Journal of the Acoustical Society of America 105: 2359–2376.

De Robertis, A., Bassett, C., Andersen, L. N., Wangen, I., Furnish, S. R., and Levine, M. 2019. Amplifier linearity accounts for discrepancies in echo-integration measurements from two widely used echosounders. ICES Journal of Marine Science, 76: 1882–1892.

De Robertis, A., and Handegard, N. O. 2013. Fish avoidance of research vessels and the efficacy of noise-reduced vessels: a review. ICES Journal of Marine Science, 70: 34–45.

De Robertis, A., Lawrence-Slavas, N., Jenkins, R., Wangen, I., Mordy, C. W., Meinig, C., Levine, M *et al.* 2019. Long-term measurements of fish backscatter from Saildrone unmanned surface vehicles and comparison with observations from a noise-reduced research vessel. ICES Journal of Marine Science, 67: 1459–1474.

De Robertis, A., McKelvey, D.R., and Ressler, P.H. 2010. Development and application of an empirical multifrequency method for backscatter classification. Canadian Journal of Fisheries and Aquatic Sciences 67: 1459–1474.

De Robertis, A., Wilson, C. D., Williamson, N. J., Guttormsen, M. A., and Stienessen, S. 2010. Silent ships sometimes do encounter more fish. 1. Vessel comparisons during winter pollock surveys. ICES Journal of Marine Science, 67: 985–995.

Dwyer, D.A., Bailey, K.M., and Livingston, P.A. 1987. Feeding habits and daily ration of walleye pollock (*Theragra chalcogramma*) in the eastern Bering Sea, with special reference to cannibalism. Canadian Journal of Fisheries and Aquatic Sciences, 44: 1972–1984.

Fässler, S.M., Brierley, A.S., and Fernandes, P.G. 2009. A Bayesian approach to estimating target strength. ICES Journal of Marine Science, 66: 1197–1204.

Foote, K.G., and Ona, E. 1985. Swim bladder cross sections and acoustic target strengths of 13 pollock and 2 saithe. Fiskeridirektoratets skrifter, Serie Havundersøkelser, 18: 1–57.

Foote, K. G. 1987. Fish target strengths for use in echo integrator surveys. The Journal of the Acoustical Society of America 82: 981–987.

Foote, K.G., and Traynor, J.J. 1988. A comparison of walleye pollock target strength estimates derived from in situ measurements and calculations based on swim bladder form. The Journal of the Acoustical Society of America, 83: 9–17.

Foote, K.G. 1983. Linearity of fisheries acoustics, with addition theorems. The Journal of the Acoustical Society of America, 73: 1932–1940.

Foote, K.G. 1991. Summary of methods for determining fish target strength at ultrasonic frequencies. ICES Journal of Marine Science 48: 211–217.

Foote, K.G., and Francis, D.T. 2002. Comparing Kirchhoff-approximation and boundary-element models for computing gadoid target strengths. The Journal of the Acoustical Society of America, 111: 1644–1654.

Fleischer, G.W., Argyle, R.L., and Curtis, G.L. 1997. In situ relations of target strength to fish size for Great Lakes pelagic planktivores. Transactions of the American Fisheries Society, 126: 786–794.

Gauthier, S., and Horne, J.K. 2004. Acoustic characteristics of forage fish species in the Gulf of Alaska and Bering Sea based on Kirchhoff-approximation models. Canadian Journal of Fisheries and Aquatic Sciences, 61: 1839–1850.

Hazen, E. L., and Horne, J. K. 2004. Comparing the modelled and measured target-strength variability of walleye pollock, *Theragra chalcogramma*. ICES Journal of Marine Science, 61: 363–377.

Horne, J.K. 2003. The influence of ontogeny, physiology, and behaviour on the target strength of walleye pollock (*Theragra chalcogramma*). ICES Journal of Marine Science, 60: 1063–1074.

Hurst, T. P. 2007. Thermal effects on behavior of juvenile walleye pollock (*Theragra chalcogramma*): implications for energetics and food web models. Canadian Journal of Fisheries and Aquatic Sciences, 64: 449–457.

Ianelli, J., Fissel, B., Holsman, K., De Robertis, A., Honkalehto, T., Kotwicki, S., Monnahan, C *et al.* 2020. Assessment of the walleye pollock stock in the eastern Bering Sea. North Pacific Stock Assessment and Fishery Evaluation Report. 173 pp. Available at https://archive.fisheries.noaa.gov/afsc/refm/stocks/plan_team/2020/EBSPollock.pdf. Last accessed 6 february 2023.

Jech, J.M., Horne, J.K., Chu, D., Demer, D.A., Francis, D.T., Gorska, N., Jones, B *et al.* 2015. Comparisons among ten models of acoustic backscattering used in aquatic ecosystem research. The Journal of the Acoustical Society of America, 138: 3742–3764.

Johnsen, E., and Godø, O.R. 2007. Diel variations in acoustic recordings of blue whiting (*Micromesistius poutassou*). ICES Journal of Marine Science, 64: 1202–1209.

Jones, D. T., Lauffenburger, N. E., Williams, K., and De Robertis, A. 2019. Results of the acoustic trawl survey of walleye pollock (*Gadus chalcogrammus*) in the Gulf of Alaska, June August 2017 (DY2017-06), AFSC Processed Rep. 2019- 08, 110 p. Alaska Fish. Sci. Cent., NOAA, Natl. Mar. Fish. Serv., 7600 Sand Point Way NE Seattle, WA 98115. https://doi.org/10.25923/89tq-ag49. last accessed 6 february 2023.

Kieser, R., Reynisson, P., and Mulligan, T. J. 2005. Definition of signal-to-noise ratio and its critical role in split-beam measurements. ICES Journal of Marine Science, 62: 123–130.

Kloser, R.J., Williams, A., and Koslow, J.A. 1997. Problems with acoustic target strength measurements of a deepwater fish, orange roughy (*Hoplostethus atlanticus*, Collett). ICES Journal of Marine Science, 54: 60–71.

Lauffenburger, N., De Robertis, A., and Kotwicki, S. 2017. Combining bottom trawls and acoustics in a diverse semipelagic environment: what is the contribution of walleye pollock (*Gadus chalcogrammus*) to near-bottom acoustic backscatter in the eastern Bering Sea? Canadian Journal of Fisheries and Aquatic Sciences, 74: 256–264.

Lavery, A. C., Bassett, C., Lawson, G. L., and Jech, J. M. 2017. Exploiting signal processing approaches for broadband echosounders. ICES Journal of Marine Science, 74: 2262–2275.

Love, R H. 1971. Dorsal-aspect target strength of an individual fish. The Journal of the Acoustical Society of America, 49: 816–823.

MacLennan, D. N., Fernandes, P. G., and Dalen, J. 2002. A consistent approach to definitions and symbols in fisheries acoustics. ICES Journal of Marine Science 59: 365–369.

MacLennan, D.N., and Menz, A. 1996. Interpretation of *in situ* target-strength data. ICES Journal of Marine Science, 53: 233–236.

Madirolas, A., Membiela, F. A., Gonzalez, J. D., Cabreira, A. G., dell'Erba, M., Prario, I. S., and Blanc, S. 2017. Acoustic target strength (TS) of argentine anchovy (*Engraulis anchoita*): the night-time scattering layer. ICES Journal of Marine Science, 74: 1408–1420.

McCarthy, A. L., Levine, M., and Jones, D. T. 2022. Results of the acoustic-trawl surveys of walleye pollock (*Gadus chalcogrammus*) in the Shumagin Islands and Shelikof Strait, February and March 2020 (DY-202001 and DY-202003). AFSC Processed Rep. 2022-08, 78 p. Alaska Fish. Sci. Cent., NOAA, Natl. Mar. Fish. Serv., 7600 Sand Point Way NE, Seattle WA 98115. https://doi.org/10.25923/r8eb-t941. last accessed 6 february 2023 .

McQuinn, I. H., and Winger, P. D. 2003. Tilt angle and target strength: target tracking of Atlantic cod (*Gadus morhua*) during trawling. ICES Journal of Marine Science, 60: 575–583.

Midttun, L. 1984. Fish and other organisms as acoustic targets. Rapp. P.-v. Reun. Cons. int. Explor. Mer 184: 25–33.

Miyanohana, Y., Ishii, K., and Furusawa, M. 1990. Measurements and analyses of dorsal-aspect target strength of six species of fish at four frequencies. Rapp. P.-v. Réun. Cons. int. Explor. Mer, 189: 317–324.

Mukai, T., and Iida, K. 1996. Depth dependence of target strength of live kokanee salmon in accordance with Boyle's law. ICES Journal of Marine Science, 53: 245–248.

Ona, E. 1990. Physiological factors causing natural variations in acoustic target strength of fish. Journal of the Marine Biological Association of the United Kingdom, 70: 107–127.

Ona, E. 1999. Methodology for Target Strength Measurements. ICES Cooperative Research Report, 235: 59

Pedersen, G., Godø, O. R., Ona, E., and Macaulay, G. J. 2011. A revised target strength–length estimate for blue whiting (*Micromesistius poutassou*): implications for biomass estimates. ICES Journal of Marine Science, 68: 2222–2228.

Core Team R. 2021. R: a language and environment for statistical computing. R Foundation for Statistical Computing, Vienna, Austria. Available from http://www.R-project.org/. last accessed 5 february 2022.

Rose, G. A. 2009. Variations in the target strength of Atlantic cod during vertical migration. ICES Journal of Marine Science, 66: 1205–1211.

Rose, G. A., and Porter, D. R. 1996. Target-strength studies on Atlantic cod (*Gadus morhua*) in Newfoundland waters. ICES Journal of Marine Science, 53: 259–265.

Rudstam, L. G., Parker-Stetter, S. L., Sullivan, P. J., and Warner, D. M. 2009. Towards a standard operating procedure for fishery acoustic surveys in the Laurentian Great Lakes, ICES Journal of Marine Science, 66: 1391–1397.

Sawada, K., Furusawa, M., and Williamson, N.J. 1993. Conditions for the precise measurement of fish target strength *in situ*. The Journal of the Marine Acoustics Society of Japan, 20: 73–79.

Sawada, K., Ye, Z., Kieser, R., McFarlane, G. A., Miyanohana, Y., and Furusawa, M. 1999. Target strength measurements and modeling of walleye pollock and Pacific hake. Fisheries science, 65: 193–205.

Simmonds, J., and MacLennan, D.N. 2008. Fisheries Acoustics: Theory and Practice. John Wiley & Sons, Oxford, UK.

Stevens, J. R., Jech, J. M., Zydlewski, G. B., and Brady, D. C. 2021. Estimating target strength of estuarine pelagic fish assemblages using fisheries survey data. The Journal of the Acoustical Society of America, 150: 2553–2565.

Stienessen, S. C., Wilson, C. D., Weber, T. C., and Parrish, J. K. 2019. External and internal grouping characteristics of juvenile walleye pollock in the Eastern Bering Sea. Aquatic Living Resources, 32: 19.

Thomas, G. L., Kirsch, J., and Thorne, R. E. 2002. Ex situ target strength measurements of Pacific herring and Pacific sand lance. North American Journal of Fisheries Management, 22: 1136–1145.

Soule, M., Barange, M., Solli, H., and Hampton, I. 1997. Performance of a new phase algorithm for discriminating between single and overlapping echoes in a split-beam echosounder. ICES Journal of Marine Science, 54: 934–938.

Traynor, J. J. 1996. Target-strength measurements of walleye pollock (*Theragra chalcogramma*) and Pacific whiting (*Merluccius productus*). ICES Journal of Marine Science, 53: 253–258.

Wall, C. C., Jech, J. M., and McLean, S. J. 2016. Increasing the accessibility of acoustic data through global access and imagery. ICES Journal of Marine Science, 73: 2093–2103.

Williams, K. 2007. Evaluation of the macroscopic staging method for determining maturity of female walleye pollock *Theragra chalcogramma* in Shelikof Strait, Alaska. Alaska Fishery Research Bulletin, 12: 252–263.

Williams, K., Punt, A. E., Wilson, C. D., and Horne, J. K. 2011. Length-selective retention of walleye pollock, *Theragra chalcogramma*, by midwater trawls. ICES Journal of Marine Science, 68: 119–129.

Yoon, E., Lee, H., Park, C., Lee, Y. D., Hwang, K., and Kim, D. N. 2023. *Ex situ* target strength of yellow croaker (*Larimichthys polyactis*) in a seawater tank. Fisheries Research, 260: 106610.

Zhao, X., Wang, Y., and Dai, F. 2008. Depth-dependent target strength of anchovy (*Engraulis japonicus*) measured *in situ*. ICES Journal of Marine Science, 65: 882–888.

Handling editor: Olav Rune Godo

Received: 13 March 2023; **Revised:** 17 May 2023; **Accepted:** 18 May 2023